

Efficiency of random search with space-dependent diffusivity

M. A. F. dos Santos¹, L. Menon Jr.¹, and C. Anteneodo^{1,2}

¹ *Department of Physics, PUC-Rio, Rua Marquês de São Vicente 225, 22451-900, Rio de Janeiro, RJ, Brazil and*

² *Institute of Science and Technology for Complex Systems, INCT-SC, Brazil*

We address the problem of random search for a target in an environment with space-dependent diffusion coefficient $D(x)$. From a general form of the diffusion differential operator that includes Itô, Stratonovich, and Hänggi-Klimontovich interpretations of the associated stochastic process, we obtain the first-passage time distribution and the search efficiency $\mathcal{E} = \langle 1/t \rangle$. For the paradigmatic power-law diffusion coefficient $D(x) = D_0|x|^\alpha$, with $\alpha < 2$, which controls whether the mobility increases or decreases with the distance from a target at the origin, we show the impact of the different interpretations. For the Stratonovich framework, we obtain a closed expression of the search efficiency, valid for arbitrary diffusion coefficient $D(x)$. We show that a heterogeneous diffusivity profile leads to lower efficiency than the homogeneous average level, and the efficiency depends only on the distribution of diffusivity values and not on its spatial organization, features that breakdown under other interpretations.

I. INTRODUCTION

In many complex environments, the diffusivity cannot be considered uniform, but changes from one point to another [1, 2]. State-dependent diffusivity has been considered to describe particles moving between nearly parallel plates [3], biologically motivated problems [4–7], and stock markets [8], among many others. Recently, heterogeneous diffusion processes (HDP) have been also investigated within the stochastic resetting scenario [9]. In one-dimension, a single trajectory $x(t)$ can be modeled by the following stochastic process

$$\dot{x} = \sqrt{2D(x)} \eta(t), \quad (1)$$

where x is the spatial coordinate (or other state variable, such as chemical coordinate or stock prize), $D(x) > 0$ is the diffusion coefficient, $\eta(t)$ is a zero-mean white noise with delta-correlation $\langle \eta(t+t')\eta(t') \rangle = \delta(t')$. Due to the white noise and multiplicative character of the stochastic Eq. (1), its integration requires an additional specification [10]. In any case, the stochastic Eq. (1) can be cast, for instance, in the Itô form, appropriate for numerical simulations, by adding a drift term, namely,

$$\dot{x} = (1 - A/2) \frac{dD(x)}{dx} + \sqrt{2D(x)} \eta(t), \quad (2)$$

where A controls the interpretation [2, 11–13]. Standard cases are $A = 0$ (Hänggi-Klimontovich or isothermal), $A = 1$ (Stratonovich), and $A = 2$ (Itô, in which case the drift term vanishes), although other values of A have also been considered [14]. For homogeneous diffusivity, the drift vanishes.

The corresponding heterogeneous diffusion equation is

$$\partial_t p(x, t) = \partial_x \left\{ D(x)^{1-A/2} \partial_x \left(D(x)^{A/2} p(x, t) \right) \right\}, \quad (3)$$

where $p(x, t)$ is the probability density function (PDF). The parameter A has impact on the spreading of particles, and can change the tails of the PDF, produce diffusion anomalies and ergodicity breaking [1, 15–17].

In Fig. 1, we show typical trajectories when the diffusivity has the power-law form $D(x) = D_0x^\alpha$, for $\alpha = \pm 0.5$ and an absorbing boundary at $x = 0$, for three different values of A . For each interpretation, the stochastic term is the same (and we used the same random sequence of the noise for comparison) but the deterministic drift term is enhanced with decreasing A . Moreover, it is either positive (if $\alpha > 0$) or negative (if $\alpha < 0$). Then, increasing A will make the walker reach the origin for the first time earlier or later, respectively, as observed in each panel of the figure.

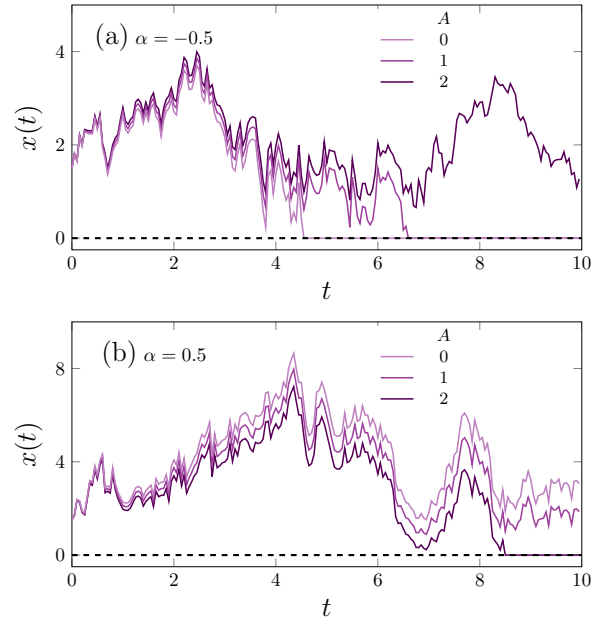


FIG. 1: Random trajectories in a heterogeneous environment with $D(x) = D_0x^\alpha$ and an absorbing boundary at $x = 0$ (dashed line), for $\alpha = -0.5$ (a) and $\alpha = 0.5$ (b). We set $D_0 = 1.0$, $x_0 = 1.5$, and the integration was performed using the stochastic Euler algorithm with time step $dt = 0.05$. In each panel, the same random sequence was used, for comparison.

Therefore, the details of a heterogeneous environment are expected to have important consequences in random searches problems [10, 18], a class of problems that is relevant in diverse contexts and at different scales [19, 20]. At the molecular level, let us mention the search of a protein for its binding site on DNA [21–23], at the ecological scales, the search for food (foraging) [24–28]. Other applications include design in robotics [29] or computer algorithms to search minima in a complex landscape [30]. In all these cases, finding efficient strategies that minimize the time to encounter the target, or optimize other search criteria, is crucial. In this context, several diffusion processes have been investigated, for instance, Lévy flights [31], fractional Brownian motion [32], Brownian search in quenched heterogeneous media [33], run-and-tumble [34], and resetting [35, 36]. Search in heterogeneous diffusivity media has been studied for particular forms of the diffusion coefficient in a confined setting, for Hänggi-Klimontovich interpretation (theoretically) [33], for Stratonovich (numerically) [37], or with stochastic resetting [38, 39]. The step shape of the diffusivity profile in a confined and d -dimensional system was investigated in Ref. [40] for all interpretations. In all these cases the mean first passage time (MFPT) was calculated, but the average of the inverse time (efficiency) is another relevant quantity, that has been calculated for instance for random search on a comb model [41]. Our purpose is to measure the search efficiency in nonconfined heterogeneous media with arbitrary diffusivity profile and arbitrary interpretation.

A target can be introduced into the diffusion equation by means of a δ -delta sink term or by absorbing boundary conditions. We will use the latter approach. Moreover, we consider that a searcher follows a HDP, exploring all points along its trajectory [19]. To study random searches, it is central to determine the first-passage-time distribution (FPTD)

$$\varphi(t) = -\frac{d}{dt}Q(x_0, t), \quad (4)$$

where $Q(x_0, t) = \int_{\Omega} p(x, t|x_0)dx$, with support Ω is the survival probability at time t . The FPTD represents the probability density of the first time the walker meets the target, after which the walker is removed from the system [10, 18]. Therefore, note that the norm of the density $p(x, t|x_0)$ is not conserved.

To quantify and compare the performance of different search processes, a fundamental measure is the so called search efficiency, and various definitions can be found in Ref. [42]. We will use a definition close to the step efficiency (inverse of the traveled time up to reaching the target) [43], namely,

$$\mathcal{E} = \langle t^{-1} \rangle = \int_0^{\infty} t^{-1} \varphi(t)dt = \int_0^{\infty} \tilde{\varphi}(s)ds, \quad (5)$$

where $\tilde{\varphi}(s)$ is the Laplace transform of the FPTD. The measure defined by Eq. (5) is adequate for systems where

the mean arrival time diverges [43]. \mathcal{E} is the first-order negative moment, which straightens the contribution of short arrival times. It has been used in a series of works to characterize the performance of Lévy searches, facing multiples targets [31], under external bias [44], comb structures [45], asymmetric Lévy flights [46] and to describe long relocations mingled with thorough local exploration [47].

Our results are organized as follows. In Sec. II, we use the backward Fokker-Planck equation, with arbitrary A , to obtain the first passage time distribution and the search efficiency when the position-dependent diffusivity has a power-law form, which has been used in different frameworks [1, 9, 48]. In Sec. III, we obtain a closed expression for the efficiency, valid for arbitrary $D(x)$, when the prescription is of Stratonovich type ($A = 1$). In all cases, examples and comparisons of the theory with stochastic simulations are provided. Final remarks are presented in Sec. IV.

II. RANDOM SEARCH IN MEDIA WITH POWER-LAW DIFFUSIVITY UNDER DIFFERENT PRESCRIPTIONS

A. Survival probability

We consider independent random walkers on a one-dimensional heterogeneous medium, initially located at position x_0 , i.e., the initial density function is $p(x, 0) = \delta(x - x_0)$ and its evolution is described by Eq. (3), which can be rewritten as

$$\begin{aligned} \frac{\partial}{\partial t}p(x, t|x_0) &= \frac{\partial^2}{\partial x^2} \{D(x)p(x, t|x_0)\} \\ &+ (A/2 - 1) \frac{\partial}{\partial x} \left\{ \frac{dD(x)}{dx} p(x, t|x_0) \right\}. \end{aligned} \quad (6)$$

In this format, the diffusion term is of the Itô form but a spurious drift term appears, which vanishes for $A = 2$. This representation will be useful to obtain the survival probability.

To address the random search problem, we consider, without loss of generality, that a target is located at $x = 0$, which corresponds to a change of coordinate. The target position defines a bound of the search domain, because we are considering a cruise search in which the walker can detect the target during its movement, and it is removed when the target is first detected. Without loss of generality, we assume that the initial position of the random searcher is $x_0 > 0$, in which case the search domain is the positive x -axis $[0, \infty)$.

Regarding the heterogeneous diffusivity, in this section we will focus our analyses on the power-law case

$$D(x) = D_0 x^{\alpha}, \quad (7)$$

where $x \geq 0$ and $\alpha < 2$. This kind of profile has been used to capture the diffusive motion of a particle on fractal objects [49] and diffusion in turbulent media [41]. It

has also been used as a paradigm of heterogeneous diffusivity to study infinite ergodic theory [17], extreme value statistics [50], and critical habitat size of biological populations [6]. In the current problem, we can interpret that the target modifies the mobility of the searcher around it, making it increase ($\alpha > 0$) or decrease ($\alpha < 0$) with distance.

The survival probability $Q(x_0, t) = \int_0^\infty p(x, t|x_0)dx$ represents the probability that the diffusing particle, starting at x_0 , has not hit the target ($x = 0$) up to time t . It can be determined through the backward Fokker-Planck equation [10], which, for the chosen power-law $D(x)$, reads

$$\begin{aligned} \frac{\partial}{\partial t} Q(x_0, t) &= D_0 x_0^\alpha \frac{\partial^2}{\partial x_0^2} Q(x_0, t) \\ &+ \frac{(1 - A/2) D_0 \alpha}{x_0^{1-\alpha}} \frac{\partial}{\partial x_0} Q(x_0, t), \end{aligned} \quad (8)$$

together with the boundary condition $Q(0, t) = 0$, meaning that the survival has null probability when the walker starts at the target position $x_0 = 0$. The initial condition is $Q(x_0 > 0, 0) = 1$, since $p(x, 0|x_0) = \delta(x - x_0)$ and $x_0 \in (0, \infty)$.

The Laplace transform, defined as $\tilde{f}(s) = \int_0^\infty f(t)e^{-st}dt$, applied on the time variable of Eq. (8), implies

$$\begin{aligned} s\tilde{Q}(x_0, s) - 1 &= D_0 x_0^\alpha \frac{\partial^2}{\partial x_0^2} \tilde{Q}(x_0, s) \\ &+ \frac{(1 - A/2) D_0 \alpha}{x_0^{1-\alpha}} \frac{\partial}{\partial x_0} \tilde{Q}(x_0, s), \end{aligned} \quad (9)$$

which can be solved analytically, as shown in Appendix A, obtaining

$$\begin{aligned} \tilde{Q}(x_0, s) &= \frac{1}{s} - \frac{2}{\Gamma[b]s} \left(\frac{x_0^{\frac{2-\alpha}{2}} \sqrt{s}}{2-\alpha} \sqrt{\frac{s}{D_0}} \right)^b \times \\ &\times K_b \left(\frac{2x_0^{\frac{2-\alpha}{2}} \sqrt{s}}{2-\alpha} \sqrt{\frac{s}{D_0}} \right), \end{aligned} \quad (10)$$

where $K_b(z)$ is the modified Bessel function and

$$b = \frac{1 - \alpha(1 - A/2)}{2 - \alpha}, \quad (11)$$

with the restriction $1 - \alpha(1 - A/2) \geq 0$. See Eq. (A11) in the appendix A.

B. First passage time distribution

From Eq. (4), the Laplace transform of the FPTD is given by $\tilde{\varphi}(s) = 1 - s\tilde{Q}(x_0, s)$, then

$$\tilde{\varphi}(s) = \left(\frac{x_0^{\frac{2-\alpha}{2}} \sqrt{s}}{2-\alpha} \sqrt{\frac{s}{D_0}} \right)^b \frac{2}{\Gamma[b]} K_b \left(\frac{2x_0^{\frac{2-\alpha}{2}} \sqrt{s}}{2-\alpha} \sqrt{\frac{s}{D_0}} \right). \quad (12)$$

To perform Laplace inversion, we use $\mathcal{L}^{-1} \left\{ s^{\frac{b}{2}} K_b(d\sqrt{s}) \right\} = \exp(-d^2/[4t]) d^b / (2t)^{b+1}$ [51], which implies

$$\varphi(t) = \frac{1}{\mathcal{Z}(2t)^{b+1}} e^{-\frac{x_0^{2-\alpha}}{(2-\alpha)^2 D_0 t}}, \quad (13)$$

with

$$\mathcal{Z}^{-1} = 2 \left(\frac{2}{2-\alpha} \right)^{2b} \frac{x_0^{1-\alpha(1-A/2)}}{(2D_0)^b \Gamma(b)}, \quad (14)$$

recalling that, from Eq. (11), it must be $\alpha(1 - A/2) < 1$, for the FPTD to be normalizable. In the particular case, $A = 2$ (Itô interpretation) and $\alpha = 1$, Eq. (13) gives $\varphi(t) = (x_0/D_0)t^{-2} \exp[-x_0/(D_0t)]$, recovering previous results [39].

Figure 2 shows the good correspondence between the obtained FPTD from the analytical prediction given by Eq. (13) and from simulations of Eq. (2) with absorbing wall at $x = 0$, for different values of A . Notice, for instance in case $\alpha = -0.5$ (a) that increasing A diminishes the probability of short times and produces longer

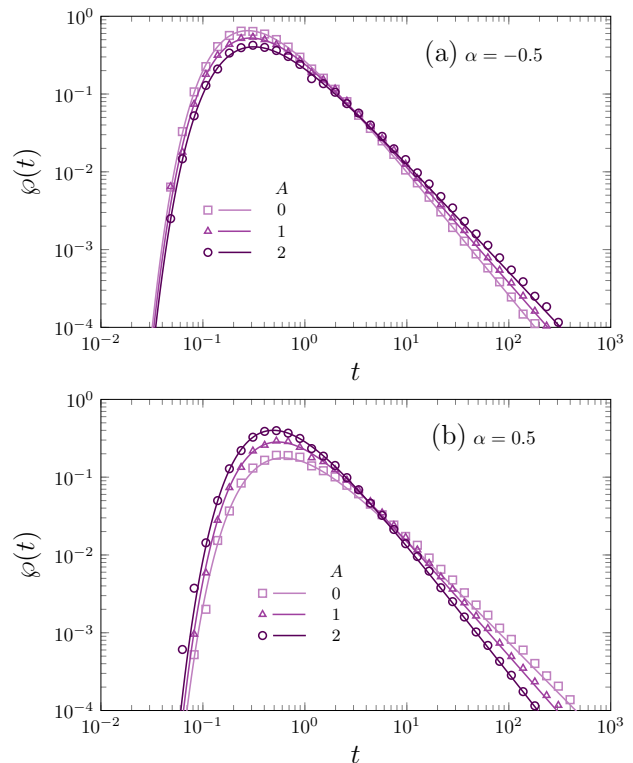


FIG. 2: First passage time distribution (FPTD) given by Eq. (13) (solid lines) and from 10^5 trajectories obtained from Eq. (2) with absorbing boundary at $x = 0$ (symbols), for the HDP with $D(x) = D_0 x^\alpha$. Panels (a) and (b) are for $\alpha = -0.5$ and $\alpha = 0.5$, respectively. In all cases $x_0 = 1.0$ and $D_0 = 1.0$. In simulations, for $t < 1$ we used $dt = 10^{-4}$, and for $t \geq 1$ we used $dt = 10^{-2}$.

tails, two features that contribute to the tendency shown in Fig. 1, delaying the encounter of the walker with the absorbing wall. The opposite occurs in case $\alpha = 0.5$ (b), also in accord with Fig. 1.

Moreover, the asymptotic behavior of $\wp(t)$ in Eq. (13) indicates that normalization is possible when $\alpha < 2$ ($A = 1, 2$) or $\alpha < 1$ ($A = 0$), which also implies the existence of the efficiency. The mean first passage time $\langle t \rangle$ is finite only for $A = 2$ and $1 < \alpha < 2$.

C. Search efficiency

The search efficiency, defined in Eq. (5), can be calculated using Eq. (12), which gives

$$\mathcal{E} = \frac{D_0}{x_0^{2-\alpha}} \left(1 - \frac{2-A}{2} \alpha \right) (2-\alpha).$$

This equation (15) summarizes the effects of the heterogeneity produced by α , under different interpretations. When $\alpha = 0$, the standard efficiency for the homogeneous case, $\mathcal{E}_H = 2D_0/x_0^2$ [31], is recovered. In Fig. 3, we show plots of \mathcal{E} as a function of α , for different values of A , generated from Eq. (15), in good agreement with the results of simulations of the stochastic Eq. (2). In Figs. 3(a)-(b), where $x_0 > 1$, we note that there is an optimal value α_{max} , which is shifted to the right with increasing A . The optimal efficiency $\mathcal{E}(\alpha_{max})$, which decays with x_0 as expected, increases with A for large enough x_0 (a) but this tendency is inverted in case (b). For $x_0 \leq 1$ (c), the efficiency monotonically decreases with α , for any A , diverging for $\alpha \rightarrow -\infty$.

As a general feature, we notice that, for fixed x_0 and fixed α , increasing A enhances the efficiency when the diffusivity increases with the distance to the target ($\alpha > 0$) but spoils the efficiency otherwise. Then, a given behavior of the diffusivity around the target (ruled by α) can be compensated by suitable correlations (ruled by A) in the motion of the searcher.

III. RANDOM SEARCH WITHIN THE STRATONOVICH SCENARIO

In this section, we consider the Stratonovich framework, for general $D(x)$. The Stratonovich HDP is the particular case of Eq. (3), setting $A = 1$, namely

$$\frac{\partial}{\partial t} p(x, t|x_0) = \frac{\partial}{\partial x} \sqrt{D(x)} \frac{\partial}{\partial x} \sqrt{D(x)} p(x, t|x_0), \quad (15)$$

with $p(\pm\infty, t|x_0) = 0$ and $p(x, 0|x_0) = \delta(x - x_0)$. This equation corresponds to the stochastic process defined by Eq. (2) with $A = 1$.

To solve the search problem, we first solve the diffusion equation (15) without a target and use the free solution to reproduce the boundary condition of the search problem through the method of images.

We introduce the following change of variables

$$y(x) = \int_0^x \frac{1}{\sqrt{D(x')}} dx', \quad (16)$$

which allows to rewrite Eq. (15) as $\partial_t \tilde{P}(y, t) = \partial_{yy}^2 \tilde{P}(y, t)$, where $\tilde{P}(y(x), t) = \sqrt{D(x)} p(x, t)$. Its natural solution, for $y \in (-\infty, \infty)$, is $\tilde{P}_0(y, t) = \exp(-y^2/(4t))/\sqrt{4\pi t}$. To reproduce an absorbing wall at the origin, i.e., $\tilde{P}(y(x=0), t) = 0$, we apply the method of images to the free

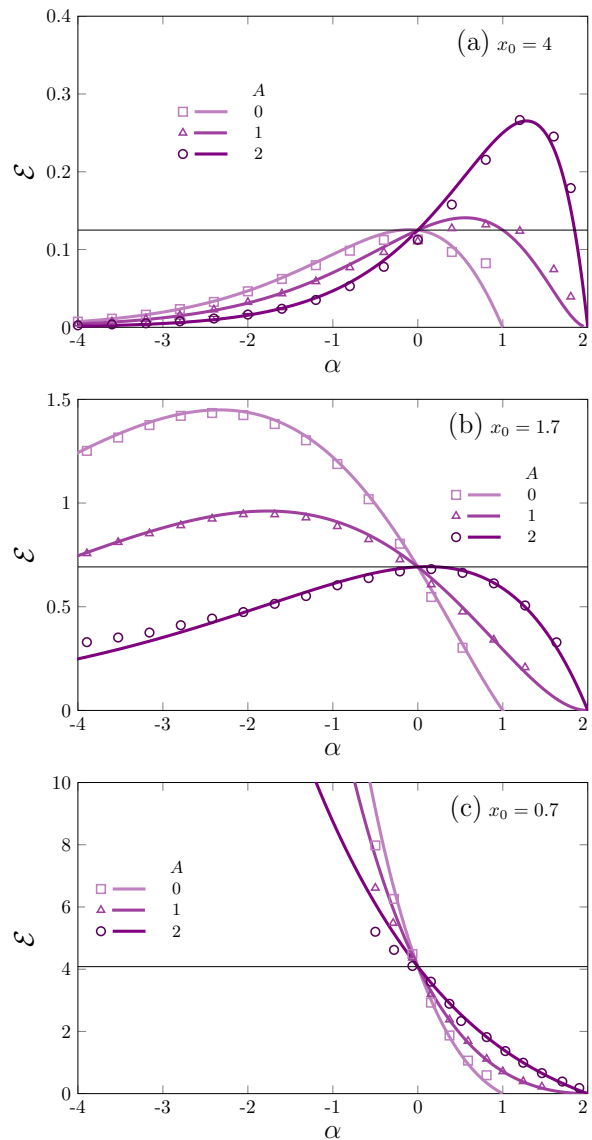


FIG. 3: Efficiency versus α for different interpretations of the HDP (values of A indicated in the legend), using $D(x) = D_0 x^\alpha$, with $D_0 = 1$. Each panel corresponds to a different value of x_0 . The prediction given by Eq. (15) is shown by solid lines, and the average over 10^5 realizations of Eq. (2) with absorbing boundary at $x = 0$ is represented by symbols. In each case, the average over is shown. The solid horizontal line corresponds to the homogeneous value $\mathcal{E}_H = 2D_0/x_0^2$.

solution with initial condition $\tilde{P}(y(x), 0) = \delta(y - y_0)$, which implies $\tilde{P}(y, t) = \tilde{P}_0(y - y_0, t) - \tilde{P}_0(y + y_0, t)$. After that, we obtain

$$p(x, t|x_0) = \frac{\tilde{P}(y, t)}{\sqrt{D(x)}} = \sum_{k=-1,1} k e^{-\frac{(y(x) - ky(x_0))^2}{4t}} \frac{1}{\sqrt{4\pi D(x)t}}. \quad (17)$$

This expression works for any space-dependent diffusivity (allowing the change $y(x)$).

An illustrative example of the PDF at a given time ($t = 1$) is presented in Fig. 4 for the power-law diffusion coefficient given by Eq. (7), with different values of α . Notice the loss of norm, visibly more pronounced with decreasing α , which favors adsorption. Besides the PDF, we show the mean square displacement (MSD) versus time. At early times, the MSD increases linearly with time for any α , meaning a normal diffusion spread. However, for long times, we observe an unusual behavior of the MSD, namely $\langle(\Delta x)^2\rangle \propto t^{\frac{2+\alpha}{2(2-\alpha)}}$. See derivation in Appendix B. When $\alpha = -2$, the MSD becomes stationary but the PDF keeps losing norm. For $\alpha < 2$, besides losing the norm, the PDF narrows with time as reflected by the negative exponent.

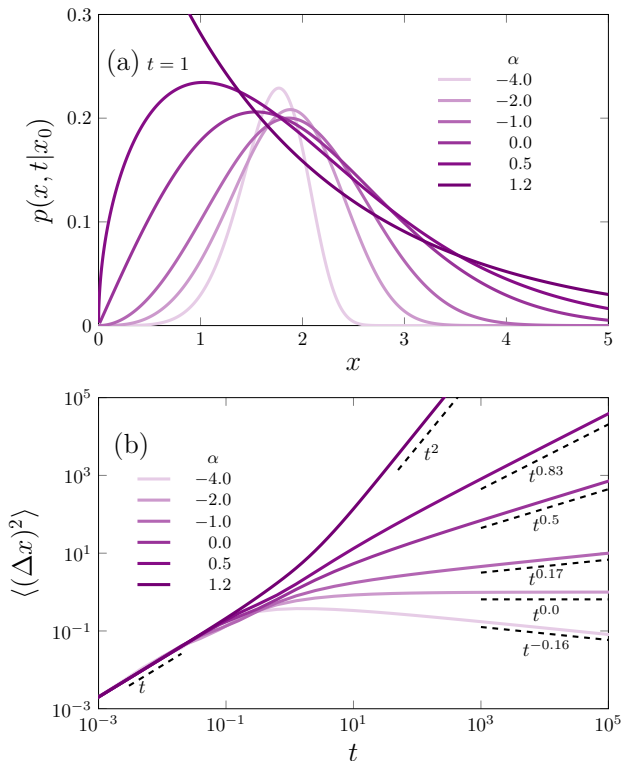


FIG. 4: (a) PDF vs. x at $t = 1$, and (b) MSD vs. t , for $D(x) = D_0 x^\alpha$, with D_0 , and different values of α indicated in the legend. In (a), the area under the curves smaller than unit is due to the loss of norm. In (b), we can observe that for short times diffusion is normal, but for long times MSD $\sim t^{\frac{2+\alpha}{2(2-\alpha)}}$.

The integration of Eq. (17) over x yields the survival probability

$$Q(x_0|t) = \int_0^\infty \frac{e^{-\frac{(y-y(x_0))^2}{4t}} - e^{-\frac{(y+y(x_0))^2}{4t}}}{\sqrt{4\pi t}} dy = \operatorname{erf}\left(\frac{y(x_0)}{2t^{\frac{1}{2}}}\right), \quad (18)$$

where erf is the error function.

The FPTD can be obtained directly from Eq. (18), using Eq. (4), namely

$$\varphi(t) = \frac{y(x_0)e^{-\frac{y(x_0)^2}{4t}}}{2\sqrt{\pi t^{\frac{3}{2}}}}. \quad (19)$$

When $D(x)$ is a power-law, we recover the result of Eq. (13) for $A = 1$.

Using $\varphi(t)$ in Eq. (19), we compute the efficiency defined in Eq. (5) $\mathcal{E} = \langle t^{-1} \rangle = \int \varphi(t)t^{-1}dt$, and through the change of variables $\xi = y_0^2/(4t)$, we have $\mathcal{E} = \frac{4}{y_0^2} \int_0^\infty \frac{e^{-\xi}}{\sqrt{\pi}} \xi^{\frac{1}{2}} d\xi = \frac{2}{y_0^2}$. Therefore,

$$\mathcal{E} = \frac{2}{\left| \int_0^{x_0} [D(x')]^{-\frac{1}{2}} dx' \right|^2}, \quad (20)$$

valid for arbitrary diffusivity profile $D(x)$. Notice that the efficiency only depends on the profile within the interval $(0, x_0)$. Moreover, notice that, since the integrand is a function of $D(x)$ only, then the efficiency does not depend on the particular sequence of values of the diffusivity. If we fragment the profile and shuffle the fragments [6], the value of the integral will be the same. This is clear if we discretize the integral in Eq. (20) as $y_0 \simeq \frac{x_0}{N} \sum_{i=1}^N [D(x_i)]^{-1/2}$, which is invariant by shuffling the values of $D(x_i)$ within the integration interval.

Moreover, to put into evidence the variations ξ around a reference level D_0 , we write $D(x) = D_0[1 + \xi(x)]$, such that $\langle \xi \rangle = 0$, and $\xi > -1$ for the positivity of D . Under such constraints for $\{\xi_i\}$, it is easy to show that $\sum_{i=1}^N [1 + \xi_i]^{-1/2}/N \geq 1$ [6], then in the continuous limit $y_0 \geq x_0/\sqrt{D_0}$, which implies

$$\mathcal{E} = \frac{2}{y_0^2} \leq \frac{2D_0}{x_0^2} = \mathcal{E}_H. \quad (21)$$

This means the remarkable property that the efficiency of a heterogeneous profile is lower than that of a homogeneous profile with a level equal to the average of the heterogeneous one.

We will provide below two concrete examples: a localized break of homogeneity, and an oscillatory profile. In addition we will discuss the case of a stochastic profile.

A. Localized heterogeneity

We analyze a profile that presents a local perturbation of the diffusivity around the level D_0 . The average

diffusivity is conserved, as far as the perturbation is contained within the interval $[0, x_0]$. The local heterogeneity depicted in Fig. 5 has width $0 \leq w \leq x_0$ and amplitude $0 \leq h \leq 1$. For this profile, Eq. (20) straightforwardly yields

$$\mathcal{E} = \frac{2D_0}{\left(x_0 - w + w \frac{\sqrt{1+h} + \sqrt{1-h}}{2\sqrt{1-h^2}}\right)^2} \leq \mathcal{E}_H. \quad (22)$$

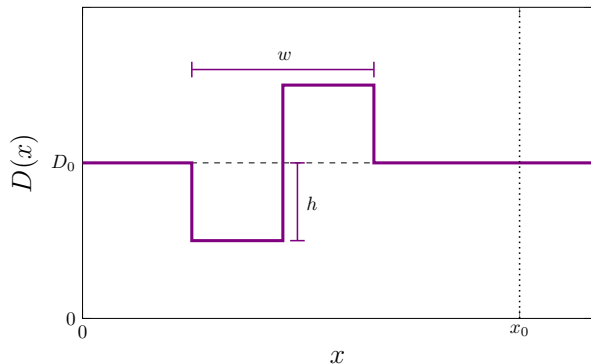


FIG. 5: Localized heterogeneity of width w and amplitude h , around the level D_0 in dashed line. The dotted vertical line highlights the initial position.

For $w = 0$ or $h = 0$, the standard value \mathcal{E}_H is recovered, while for increasing w and $|h|$, the efficiency decays, as can be visualized in Fig. 6. This means that, in a heterogeneous profile that preserves the average, the search is less efficient than in an homogeneous environment with the average diffusivity. Let us also note, from Eq. (20), that a rigid shift of the pulse will not affect the efficiency, as soon as the pulse remains contained within the integration interval $[0, x_0]$. Also, fragmentation of the pulse into smaller ones will produce the same result, as far as the total length of up and down diffusivities is the same. This property is related to the Stratonovich prescription

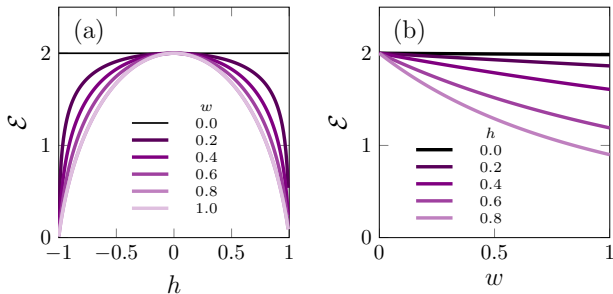


FIG. 6: Efficiency for the landscape sketched in Fig. 5, varying h and w . Notice that in all cases the efficiency is lower than that for the homogeneous case. The horizontal lines correspond to \mathcal{E}_H the value for the homogeneous case with same average.

and does not apply to other values of $A \neq 1$, as we will exemplify below.

B. Oscillating diffusivity

As a paradigm of an oscillatory landscape, we analyze the sinusoidal diffusivity kernel

$$D(x) = D_0 [1 + d \cos(kx)], \quad (23)$$

where oscillations occur around the reference level D_0 , with $-1 \leq d \leq 1$ and wavenumber k . We integrated numerically the general expression for the efficiency, Eq. (20), using $D(x)$ in Eq. (23), showing the results in Fig. 7.

For a fair comparison with the homogeneous case, let us consider oscillations whose average around D_0 vanishes. This occurs when $kx_0 = N\pi$, with integer N , and also in the limit of very short wavelength compared to x_0 (i.e., $\lambda = 2\pi/k \ll x_0$). For integer N , we obtain

$$\mathcal{E}_0 \simeq \mathcal{E}_H \frac{(1+d)\pi^2}{4[\kappa(\frac{2d}{1+d})]^2} \leq \mathcal{E}_H, \quad (24)$$

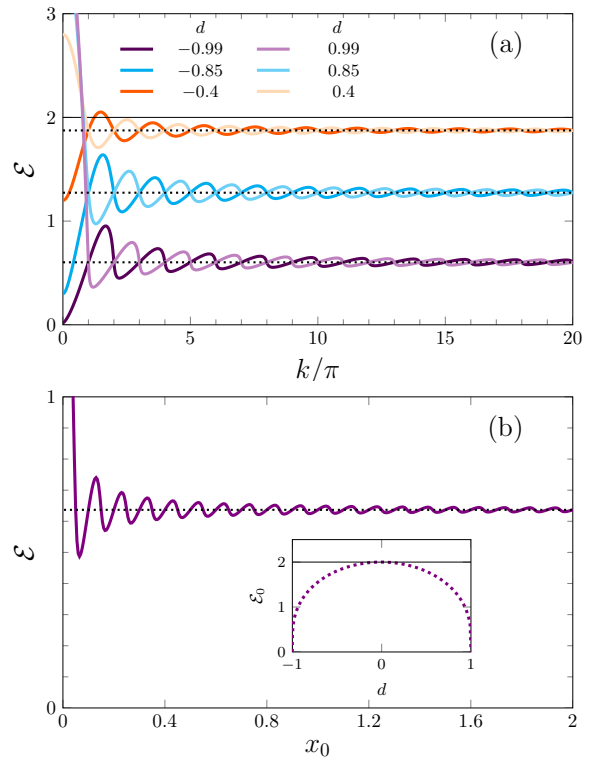


FIG. 7: (a) Efficiency \mathcal{E} for $D(x) = D_0[1 + d \cos(kx)]$ versus k , for different values of d . The dotted horizontal lines correspond to the respective short-wavelength limit given by Eq. (24). We set $x_0 = 1$ and $D_0 = 1$. In (b), we plot the short-wavelength limit \mathcal{E}_0 (dashed line) vs. d , and for comparison, the efficiency of the corresponding homogeneous case \mathcal{E}_H (thin horizontal line). In the inset we plot $\mathcal{E}/\mathcal{E}_H$ versus x_0 , for $k = 20\pi$, $D_0 = 1$ and $d = 0.85$.

where $\kappa(z) = \frac{\pi}{2} {}_2F_1(\frac{1}{2}, \frac{1}{2}, 1, z)$ is the complete elliptic integral of the first kind. The short-wavelength limit \mathcal{E}_0 , for each d , is plotted in Fig. 7 by dotted horizontal lines. Notice that, in fact, it is attained for integer N or large k . This limit value is independent of the introduction of a phase constant in Eq. (23), as can be observed when d changes sign. More importantly, Eq. (24) is maximal at $d = 0$ where it takes the value \mathcal{E}_H . That is, the efficiency \mathcal{E}_0 remains below that of the homogeneous case with the same average diffusivity. This is a noticeable result that indicates that short-wavelength oscillations of the diffusivity spoil the efficiency of the search, which decays with increasing d , as represented by the dashed line in Fig. 7(b). In contrast, for small values of k , the value of the efficiency can be higher than \mathcal{E}_H , but this simply reflects an average diffusivity higher than D_0 .

C. Random diffusivity

As discussed in connection with Eq. (21), shuffled diffusivity profiles in the interval $(0, x_0)$ yield the same efficiency within Stratonovich framework. This leads to consider noisy diffusivity profiles $D(x) = D_0(1 + \xi)$, around the level D_0 , taking uncorrelated random values ξ with a given PDF $f(\xi)$, where $\xi \in (-1, \infty)$, such that the average $\langle \xi \rangle = \int_{-1}^{\infty} \xi f(\xi) d\xi = 0$. Following this idea, Eq. (20) can be rewritten as

$$\mathcal{E} = \frac{\mathcal{E}_H}{\left(\int_{-1}^{\infty} [1 + \xi]^{-\frac{1}{2}} f(\xi) d\xi \right)^2} \leq \mathcal{E}_H, \quad (25)$$

where upper bound comes from the inequality [6]

$$\int_{-1}^{\infty} [1 + \xi]^{-\frac{1}{2}} f(\xi) d\xi \geq 1. \quad (26)$$

Considering, that $\xi(x) = D(x)/D_0 - 1$, where x can be interpreted as a random variable that is uniform in the interval $[0, x_0]$, through the change-of-variables method, we can obtain $f(\xi)$. For instance, in the case of $D(x) = D_0[1 + d \cos(n\pi x/x_0)]$, considered in Section III B, it is $f(\xi) = [1 - \xi^2/d^2]^{-\frac{1}{2}}/(\pi d)$, for $\xi \in (-d, d)$, which substituted into Eq. (25) allows to reobtain Eq. (24).

D. Comparison with other interpretations

In the precedent results of Sec. III, we presented results for arbitrary $D(x)$ within Stratonovich interpretation. We will perform a comparison with other interpretations using the profile $D(x) = D_0[1 + d \cos(kx/x_0)]$ through simulations of the stochastic differential Eq. (2), calculating and plotting the efficiency vs. d in Fig. 8. We consider cases where $k/x_0 = n\pi$ with integer n , hence the average level is D_0 .

In Fig. 8(a), where monotonic profiles are used, we can observe several features. For $A = 1$, the efficiency is

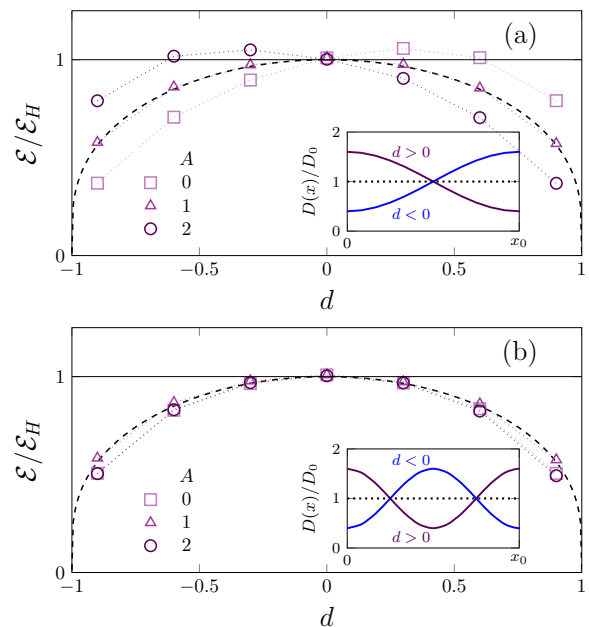


FIG. 8: Relative efficiency $\mathcal{E}/\mathcal{E}_H$ vs. d for the profile $D(x) = D_0[1 + d \cos(kx/x_0)]$ using different interpretations (values of A), for (a) $k/x_0 = \pi$ and (b) $k/x_0 = 2\pi$. In both cases the prediction given by Eq. (24) for the Stratonovich case (dashed line) and the homogeneous value (horizontal full line), both normalized by \mathcal{E}_H are plotted. Symbols correspond to the average over 10^5 trajectories of Eq. (2), with absorbing boundary at $x = 0$. The diffusivity profiles are depicted in the insets.

insensitive to the ordering as proved throughout this section, then there is a symmetry of inversion $d \rightarrow -d$. However, notice that this symmetry is broken for the other interpretations, meaning that the shape of the profile and only the distribution of values are relevant. Moreover, we observe that when the profile increases with the distance from the target ($d < 0$), the efficiency increases with A , while the contrary occurs for a decreasing profile ($d > 0$). Actually, this is the same behavior demonstrated analytically for the power-law case analyzed in Sec. II. Finally note that while for $A = 1$ the efficiency remains below that of the homogeneous profile, this can be violated for the other interpretations.

In Fig. 8(b), where the diffusivity profiles are not monotonic, the efficiency appears to be symmetric around $d = 0$, and smaller for $A \neq 1$ than for $A = 1$.

IV. FINAL REMARKS

We have obtained the efficiency of the search problem when the medium is heterogeneous. For general interpretations characterized by parameter A , we developed the paradigmatic case with power-law diffusivity with exponent $\alpha < 2$, which embraces the cases with increasing and decreasing mobility with the distance from the tar-

get. We observed that depending on the initial position of the searcher, there can be an optimal value of α , which depends on A . But a finite maximum not always occurs. The general feature is that, increasing A favors the search when the diffusivity increases with the distance from the target ($\alpha > 0$) and hinders the search otherwise. Moreover, this is not unique to the power-law shape but is determined by the monotonic character.

The different interpretations represented by A produce qualitatively similar pictures. Then, we considered the Stratonovich framework ($A = 1$) that allows deriving a closed expression of the efficiency for arbitrary forms of $D(x)$. In this case, we considered a localized perturbation and an oscillatory one, concluding that these heterogeneities spoil the efficiency of the homogeneous case with a level equal to the average one. It is important to note that the shape of the diffusivity profile within the search interval is not relevant but only the set of values of the profile, which determine the integral in Eq. (20). This is a property analogous to that found in the context of critical patch size [6]. Therefore, a noisy profile with the same distribution of values yields the same results. However, for other interpretations other than Stratonovich one, the shape of the profile (not only the distribution of values) is relevant.

As a perspective, it would be interesting to extend the present study to higher dimensions and confined systems. We want to call the attention that our results can be applied to the problem of the first encounter between two walkers $x(t)$ and $y(t)$, with a coupled diffusivity depending on their distance $D(|x - y|)$. For $x_0 > y_0$, $z(t) = x(t) - y(t) > 0$, and for $z(t) = 0$ the first encounter occurs [52, 53]. In such case, the efficiency measures the rate of success of the first encounter.

Acknowledgments: We acknowledge partial financial support by the Coordenação de Aperfeiçoamento de Pessoal de Nível Superior - Brazil (CAPES) - Finance Code 001. C.A. also acknowledges partial support by Conselho Nacional de Desenvolvimento Científico e Tecnológico (CNPq), and Fundação de Amparo à Pesquisa do Estado do Rio de Janeiro (FAPERJ).

Appendix A: Solving Eq. (9)

First, we introduce the new function

$$\tilde{q}(x_0, s) = \tilde{Q}(x_0, s) - \frac{1}{s}, \quad (\text{A1})$$

into Eq. (9), obtaining

$$\begin{aligned} \frac{\partial^2}{\partial x_0^2} \tilde{q}(x_0, s) + \left(1 - \frac{A}{2}\right) \frac{\alpha}{x_0} \frac{\partial}{\partial x_0} \tilde{q}(x_0, s) \\ - \frac{s}{D_0 x_0^\alpha} \tilde{q}(x_0, s) = 0. \end{aligned} \quad (\text{A2})$$

Using the change of variables

$$\begin{aligned} z &= \sqrt{x_0} \\ \tilde{q}(x_0, s) &= z^\nu \tilde{w}(z, s), \end{aligned}$$

in Eq. (A2), we get

$$\begin{aligned} \frac{\partial^2}{\partial z^2} \tilde{w}(z, s) + \frac{\mathcal{A}}{z} \frac{\partial}{\partial z} \tilde{w}(z, s) \\ + \left(\frac{\mathcal{B}}{z^2} - \left(2 \frac{\sqrt{s}}{\sqrt{D_0} z^{\alpha-1}} \right)^2 \right) \tilde{w}(z, s) = 0, \end{aligned} \quad (\text{A3})$$

where $\mathcal{A} = 2\nu - 1 + (1 - A/2)2\alpha$ and $\mathcal{B} = \nu(\nu - 2 + 2\alpha(1 - A/2))$. Equation (A3) can be identified with a Lommel-type equation [54], which admits the solution

$$\tilde{w}(z, s) = c_1 z^\beta K_b [az^{2-\alpha}] + c_2 z^\beta I_b [az^{2-\alpha}], \quad (\text{A4})$$

where $K_b(\dots)$ and $I_b(\dots)$ are the modified Bessel functions [51],

$$a = \frac{2}{2-\alpha} \sqrt{\frac{s}{D_0}}, \quad (\text{A5})$$

$$\beta = 1 - \nu - \alpha(1 - A/2), \quad (\text{A6})$$

$$b = \pm[1 - \alpha(1 - A/2)]/(2 - \alpha), \quad (\text{A7})$$

here the \pm can be ignored since $K_b(z) = K_{-b}(z)$. To ensure the convergence of the solution $\tilde{w}(z, s)$, for large z , we must set $c_2 = 0$ into the Eq. (A4). Therefore, according Eq. (16) $\tilde{q}(x_0, s) = z^\nu w(z, s)$, we obtain

$$\tilde{q}(x_0, s) = c_1 x_0^{\frac{1}{2}(1-\alpha[1-A/2])} K_b \left(\frac{2x_0^{\frac{2-\alpha}{2}} \sqrt{s}}{2-\alpha} \sqrt{\frac{s}{D_0}} \right). \quad (\text{A8})$$

The probability of survival in Laplace space (see Eq. (A1)) is given by

$$\tilde{Q}(x_0, s) = c_1 x_0^{\frac{1}{2}(1-\alpha[1-A/2])} K_b \left(\frac{2x_0^{\frac{2-\alpha}{2}} \sqrt{s}}{2-\alpha} \sqrt{\frac{s}{D_0}} \right) + \frac{1}{s},$$

where the coefficient c_1 is obtained from the boundary condition $\tilde{Q}(x_0 = x_a, s) = 0$, where x_a is the target position. Then

$$\tilde{Q}(x_0, s) = \frac{1}{s} \left[1 - \frac{x_0^{\frac{1}{2}(1-\alpha[1-A/2])} K_b \left(\frac{2x_0^{\frac{2-\alpha}{2}} \sqrt{s}}{2-\alpha} \sqrt{\frac{s}{D_0}} \right)}{x_a^{\frac{1}{2}(1-\alpha[1-A/2])} K_b \left(\frac{2x_a^{\frac{2-\alpha}{2}} \sqrt{s}}{2-\alpha} \sqrt{\frac{s}{D_0}} \right)} \right],$$

taking the limit $x_a \rightarrow 0$ in the part of function that contain the x_a parameter, we obtain

$$\begin{aligned} \mathcal{I} &= \lim_{x_a \rightarrow 0} x_a^{\frac{1}{2}(1-\alpha[1-A/2])} K_b \left(\frac{2x_a^{\frac{2-\alpha}{2}} \sqrt{s}}{2-\alpha} \sqrt{\frac{s}{D_0}} \right) \\ &\simeq \lim_{x_a \rightarrow 0} x_a^{\frac{1}{2}(1-\alpha[1-A/2])} \frac{\Gamma[b]}{2^{1-b}} \left(\frac{2x_a^{\frac{2-\alpha}{2}} \sqrt{s}}{2-\alpha} \sqrt{\frac{s}{D_0}} \right)^{-b} \\ &= \lim_{x_a \rightarrow 0} x_a^{\frac{2-\alpha}{2} \left(\frac{1-\alpha[1-A/2]}{2-\alpha} - b \right)} \frac{\Gamma[b]}{2^{1-b}} \left(\frac{2}{2-\alpha} \sqrt{\frac{s}{D_0}} \right)^{-b} \\ &= \frac{\Gamma[b]}{2^{1-b}} \left(\frac{2}{2-\alpha} \sqrt{\frac{s}{D_0}} \right)^{-b}, \end{aligned} \quad (\text{A9})$$

which is non null only for $b = [1 - \alpha(1 - A/2)]/(2 - \alpha)$.

Therefore,

$$\begin{aligned} \tilde{Q}(x_0, s) &= \quad (A10) \\ &= \frac{1}{s} \left[1 - \frac{2}{\Gamma[b]} \left(\frac{x_0^{\frac{2-\alpha}{2}}}{2-\alpha} \sqrt{\frac{s}{D_0}} \right)^b K_b \left(\frac{2x_0^{\frac{2-\alpha}{2}}}{2-\alpha} \sqrt{\frac{s}{D_0}} \right) \right]. \end{aligned}$$

The FPTD in Eq. (A10) is normalized only for $b > 0$, then

$$1 - \alpha(1 - A/2) \geq 0. \quad (A11)$$

Appendix B: Mean square displacement (MSD)

We calculate the second moment, which determines the asymptotic long-time limit presented in Fig. 4. To do that we perform the average using Eq. (17) as

$$\begin{aligned} \mathcal{L}\{\langle x^2 \rangle\} &= \int_0^\infty x^2 p(x, t) dx \\ &= \int_0^\infty \frac{x^{2-\frac{\alpha}{2}}}{\sqrt{4s}} \left(e^{-\sqrt{s}|y(x)-y(x_0)|} - e^{-\sqrt{s}|y(x)+y(x_0)|} \right) dx \\ &= e^{-\sqrt{s}y(x_0)} \int_0^{x_0} \frac{x^{2-\frac{\alpha}{2}}}{\sqrt{4s}} e^{\sqrt{s}y(x)} dx \\ &\quad + e^{\sqrt{s}y(x_0)} \int_{x_0}^\infty \frac{x^{2-\frac{\alpha}{2}}}{\sqrt{4s}} e^{-\sqrt{s}y(x)} dx \\ &\quad - e^{-\sqrt{s}y(x_0)} \int_0^\infty \frac{x^{2-\frac{\alpha}{2}}}{\sqrt{4s}} e^{-\sqrt{s}y(x)} dx \\ &= \frac{\sinh(\sqrt{s}y(x_0))}{\sqrt{s}} \int_{x_0}^\infty x^{2-\frac{\alpha}{2}} e^{-\sqrt{s}y(x)} dx, \quad (B1) \\ &\quad + \frac{e^{-\sqrt{s}y(x_0)}}{\sqrt{s}} \int_0^{x_0} x^{2-\frac{\alpha}{2}} \sinh(\sqrt{s}y(x)) dx, \end{aligned}$$

where y was defined in Eq. (16). Defining $z = \sqrt{s}y$ we get

$$z(x) = 2s^{\frac{1}{2}} x^{1-\frac{\alpha}{2}} / (2 - \alpha), \quad (B2)$$

which implies $x = c_\alpha (z/\sqrt{s})^{\frac{2}{2-\alpha}}$ with $c_\alpha = \left(\frac{2-\alpha}{2}\right)^{\frac{2}{2-\alpha}}$.

$$\begin{aligned} \mathcal{L}\{\langle x^2 \rangle\} &= c_\alpha^2 \frac{\sinh(\sqrt{s}y(x_0))}{s^{\frac{4-\alpha}{2-\alpha}}} \int_{\sqrt{s}y_0}^\infty z^{\frac{4}{2-\alpha}} e^{-z} dz. \\ &\quad + c_\alpha^2 \frac{e^{-\sqrt{s}y(x_0)}}{s^{\frac{4-\alpha}{2-\alpha}}} \int_0^{\sqrt{s}y_0} z^{\frac{4}{2-\alpha}} \sinh(z) dz \quad (B3) \end{aligned}$$

where $z(x_0) = \sqrt{s}y(x_0) \equiv \sqrt{s}y_0$.

For large t , i.e., $s \sim 0$, the first term in Eq. (B3) dominates and we obtain

$$\begin{aligned} \mathcal{L}\{\langle x^2 \rangle\} \Big|_{s \sim 0} &\simeq \frac{c_\alpha^2 y_0}{(\sqrt{s})^{\frac{6-\alpha}{2-\alpha}}} \int_0^\infty z^{\frac{4}{2-\alpha}} e^{-z} dz \\ &\simeq \frac{2y_0 c_\alpha^{1+\frac{\alpha}{2}} \Gamma\left[\frac{4}{2-\alpha}\right]}{(\sqrt{s})^{\frac{6-\alpha}{2-\alpha}}}. \quad (B4) \end{aligned}$$

Therefore, we obtain the asymptotic behavior

$$\langle x^2 \rangle \simeq \frac{2y_0 c_\alpha^{1+\frac{\alpha}{2}} \Gamma\left[\frac{4}{2-\alpha}\right]}{\Gamma\left[\frac{1}{2} \frac{6-\alpha}{2-\alpha}\right]} t^{\frac{2+\alpha}{2(2-\alpha)}} \sim t^{\frac{2+\alpha}{2(2-\alpha)}}. \quad (B5)$$

Notice that for $\alpha = 0$, normal diffusion is not obtained, due to the presence of the absorbing wall [18].

-
- [1] A. G. Cherstvy, A. V. Chechkin and R. Metzler, *New J. Phys.* **15**, 083039 (2013).
[2] G. Pesce, A. McDaniel, S. Hottovy, J. Wehr and G. Volpe, *Nat. Commun.* **4**, 1-7 (2013).
[3] P. Lançon, G. Batrouni, L. Lobry, and N. Ostrowsky, *Europhys Lett.* **54**, 28 (2001).
[4] S. Pieprzyk, D. Heyes and A. Brańka, *Biomicrofluidics* **10**, 054118 (2016).
[5] A. Berezhkovskii and D. Makarov, *J. Chem. Phys.* **147**, 201102 (2017).
[6] M. A. F. dos Santos, V. Dornelas, E. H. Colombo and C. Anteneodo, *Phys. Rev. E* **102**, 042139 (2020).
[7] M. A. F. dos Santos, E. H. Colombo and C. Anteneodo, *Chaos Solitons Fractals* **152** pp. 111422 (2021).
[8] B. Oksendal, *Stochastic differential equations: an introduction with applications* (Springer Science & Business Media, 2013).
[9] T. Sandev, V. Domazetoski, L. Kocarev, R. Metzler and A. Chechkin, *J. Phys. A Math.* **55**, 074003 (2022).
[10] H. Risken, *The Fokker-Planck Equation*, 2nd ed. (Springer-Verlag, Berlin, 1989).
[11] P. Hänggi, *Phys. Rev. A* **25**, 1130 (1982).
[12] R. L. Stratonovich, *SIAM Journal On Control* **4**, 362-371 (1966).
[13] K. Itô, *Proc. Imp. Acad.* **20**, 519-524 (1944).
[14] S. Hottovy, G. Volpe and J. Wehr, *J. Stat. Phys.* **146**, 762-773 (2012).
[15] M. A. F. dos Santos and I. S. Gomez, *J. Stat. Mech.: Theory Exp.* **2018**, 123205 (2018).
[16] P. C. Bressloff and S. D. Lawley, *Phys. Rev. E* **95**, 060101(R) (2017).
[17] N. Leibovich and E. Barkai, *Phys. Rev. E* **99**, 042138 (2019).
[18] S. Redner, *A guide to first-passage processes* (Cambridge university press, 2001).
[19] O. Bénichou, C. Loverdo, M. Moreau and R. Voituriez, *Rev. Mod. Phys.* **83**, 81 (2011).
[20] V. Zaburdaev, S. Denisov and J. Klafter, *Rev. Mod.*

- Phys.* **87**, 483 (2015).
- [21] L. Mirny, M. Slutsky, Z. Wunderlich, A. Tafvizi, J. Leith and A. Kosmrlj, *J. Phys. A Math.* **42**, 434013 (2009).
- [22] X. Chen, X. Cheng, Y. Kang, and J. Duan, *J. Stat. Mech.: Theory Exp.* **2019**, 033501 (2019).
- [23] A. Bhattacharjee and Y. Levy, *Nucleic Acids Res.* **42**, 12404-12414 (2014).
- [24] W. J. O'Brien, H. I. Browman and B. I. Evans, *Am. Sci.* **78**, 152-160 (1990).
- [25] G. M. Viswanathan, S. V. Buldyrev, S. Havlin, M. G. E. da Luz, E. P. Raposo and H. E. Stanley, *Nature* **401**, 911-914 (1999).
- [26] G. M. Viswanathan, V. Afanasyev, S. V. Buldyrev, S. Havlin, M. G. E. da Luz, Raposo, E. and H. E. Stanley, *Phys. A: Stat. Mech. Appl.* **295**, 85-88 (2001).
- [27] F. Bartumeus, M. G. e. da Luz, G. M. Viswanathan and J. Catalan, *Ecology* **86**, 3078-3087 (2005)
- [28] G. M. Viswanathan, M. G. E. da Luz, E. P. Raposo, and H. E. Stanley, *The physics of foraging: an introduction to random searches and biological encounters* (Cambridge University Press, 2011).
- [29] E. Castello, T. Yamamoto, F. D. Libera, W. Liu, A. F. Winfield, Y. Nakamura and H. Ishiguro, *Swarm Intell.* **10**, 1-31 (2016).
- [30] I. Pavlyukevich, *J. Comput. Phys.* **226**, 1830-1844 (2007).
- [31] V. V. Palyulin, V. N. Mantsevich, R. Klages, R. Metzler and A. V. Chechkin, *Eur. Phys. J. B* **90**, 1-16 (2017).
- [32] S. M. Khadem, S. H. L. Klapp and R. Klages, *Phys. Rev. Res.* **3**, 023169 (2021).
- [33] A. Godec and R. Metzler, *Phys. Rev. E* **91**, 052134 (2015).
- [34] J. F. Rupprecht, O. Bénichou and R. Voituriez, *Phys. Rev. E* **94**, 012117 (2016).
- [35] A. Chechkin and I. M. Sokolov, *Phys. Rev. Lett.* **121**, 050601 (2018)
- [36] U. Bhat, C. De Bacco and S. Redner, *J. Stat. Mech.: Theory Exp.* **2016**, 083401 (2016).
- [37] N. M. Mutothya, Y. Xu, Y. Li, R. Metzler and N. M. Mutua, *J. phys. Complex* **2**, 045012 (2021).
- [38] M. K. Lenzi, E. K. Lenzi, L. M. S. Guilherme, L. R. Evangelista and H. V. Ribeiro, *Phys. A: Stat. Mech. Appl.* **588**, 126560 (2022).
- [39] S. Ray, *J. Chem. Phys.* **153**, 234904 (2020).
- [40] G. Vaccario, C. Antoine and J. Talbot *Phys. Rev. Lett.* **115**, 240601 (2015).
- [41] T. Sandev, A. Iomin and L. Kocarev, *Phys. Rev. E* **102**, 042109 (2020).
- [42] A. James, J. W. Pitchford and M. J. Plank, *Bull. Math. Biol.* **72**, 896-913 (2010).
- [43] V. V. Palyulin, A. V. Chechkin and R. Metzler, *Proc. Natl. Acad. Sci. U. S. A.* **111**, 2931-2936 (2014).
- [44] V. V. Palyulin, A. V. Chechkin and R. Metzler, *J. Stat. Mech.: Theory Exp.* **2014**, P11031 (2014).
- [45] T. Sandev, A. Iomin, and L. Kocarev, *J. Phys. A Math.* **52**, 465001 (2019).
- [46] A. Padash, T. Sandev, H. Kantz, R. Metzler and A. V. Chechkin, *Fractal And Fractional* **6**, 260 (2022).
- [47] V. V. Palyulin, A. V. Chechkin, R. Klages and R. Metzler, *J. Phys. A Math.* **49**, 394002 (2016).
- [48] T. Sandev, A. Schulz, H. Kantz and A. Iomin, *Chaos Solitons Fractals* **114**, 551-555 (2018).
- [49] B. O'Shaughnessy and I. Procaccia, *Phys. Rev. Lett.* **54**, 455-458 (1985).
- [50] P. Singh, *Phys. Rev. E* **105**, 024113 (2022).
- [51] M. Abramowitz, *Handbook of mathematical functions with formulas Graphs, and Mathematical Tables* (1965).
- [52] F. Le Vot, S. B. Yuste, E. Abad and D. S. Grebenkov, *ArXiv Preprint arXiv:2201.05388*, (2022).
- [53] F. Le Vot, S. B. Yuste, E. Abad and D. S. Grebenkov, *Phys. Rev. E* **102**, 032118 (2020).
- [54] I. S. Gradshteyn, I. M. Ryzhik, A. Jeffrey and D. Zwillinger, *Table of Integrals, Series, and Products. Table of Integrals* (2007).